SPPT 2004

Proceedings of the

21st Symposium on PLASMA PHYSICS AND TECHNOLOGY

Prague, Czech Republic,
June 14-17, 2004

CZECHOSLOVAK
JOURNAL
OF
PHYSICS

Vol. 54 2004 Suppl. C

CZYPAO 54 (C) C1-C1073 (2004) ISSN 0011-4626

Recognized by the
EUROPEAN PHYSICAL SOCIETY

Generation of microdischarges in porous materials

K. Hensel

Comenius University, Faculty of Mathematics, Physics and Informatics, Department of Plasma Physics, 842–48 Mlynská dolina, Bratislava, Slovakia
e-mail: hensel@fmph.uniba.sk

Y. Matsui, S. Katsura, A. Mizuno

Toyohashi University of Technology, Department of Ecological Engineering, Tempaku-cho, 441-8580 Toyohashi, Japan

Received 24 April 2004

Formation of microdischarges in porous dielectric materials generated by dc high voltage has been investigated. Two geometrical configurations (sandwich type and corona type) and several materials with different pore size and thickness have been tested. The I–V characteristics and current pulse characteristics have been recorded and supplemented with the photographs of the discharge. Stable microdischarges have been successfully generated only using materials with a certain pore size and in the limited range of the I–V characteristics.

PACS: 52.80.Tn
Key words: microdischarge, porous ceramics

1 Introduction

Non–thermal plasmas are emerging as successful methods to convert various gaseous pollutants into inert or treatable species [1, 2]. Chemical reactions in the plasmas are mainly initiated by the interaction of molecules with energetic electrons produced by various electrical discharges and the free radicals. To improve the energy efficiency and selectivity of non–thermal plasma applications, combination of non–thermal plasma and catalyst has been investigated recently [3, 4]. Various materials including dielectrics, ferroelectrics and metals oxides are used as catalysts, which can improve the formation of active radicals and their distribution. The presence of the catalyst in the reactor also influences the discharge plasma modes and their electrical characteristics. In the ferroelectric–bed discharge (FBD), a material with high permittivity (ferroelectric pellets of e. g. $BaTiO_3$, $PbTiO_3$) is held between two electrodes. Once the high voltage is applied, the electric field at the contact points of the pellets is enhanced and a discharge occurs. The discharge consists of a large number of intermittent breakdown filaments, microdischarges, occurring especially in the vicinity of the contact points. Filamentary microdischarge can also be observed in a dielectric–barrier discharge (DBD) between two electrodes, at least one of which is covered with a dielectric (e.g. quartz, ceramics and polymers). A large number of filamentary microdischarges of nanosecond duration randomly distributed both in time and in space appears upon the breakdown. Their number is proportional to the voltage applied on the electrodes and the frequency is usually of several hundreds kHz [5, 6]. The microdischarges of FBD and DBD are excellent sources of energetic electrons and free radicals of a high density. Due to its attractive properties, the microdischarge phenomenon is studied

for potential industrial applications, e.g. ozone generators, free radical generation and their applications in pollution control.

In this paper, we present experimental investigations of the microdischarges formation in porous dielectric materials. The aim of this study is to determine the conditions of discharge generation with respect to the pore size and thickness of the dielectric material. The discharge in two different geometry configurations has been generated. Although ac or pulsed high voltage power is typically needed in both ferroelectric and dielectric barrier discharges to generate microdischarges, we have instead successfully used the dc power. The generation of the microdischarges inside the porous media is interesting from the point of view of car industry, where ceramic honeycomb catalysts are used for engine exhaust abatement. Although it is quite difficult to generate uniform non–thermal discharge plasma inside narrow holes of the ceramic honeycomb catalyst [7], finding an effective combination of plasma and honeycomb catalyst and improving the performance is a challenge.

2 Experimental setup

A schematic diagram of the experimental apparatus is shown in Fig. 1. The first configuration (sandwich geometry, 1a) employs the dielectric placed between two mesh electrodes (∅ 14 mm). Fig. 2 summarizes the physical properties and shapes of the used dielectrics. The diameter of the dielectrics was 28 mm and their thickness was 3 and 6 mm for A, B, C and D, E, respectively. The ceramics A, B, C were sintered from alumina (Al_2O_3) powder particles of different sizes and the ceramics D and E were made of cordierite ($2MgO.2Al_2O_3.5SiO_2$) and alumina. In the second configuration (corona geometry, 1b), the dielectric was placed on the mesh electrode with multi–point electrode above consisted of 5 nails in one row placed 25 mm above the grounded mesh electrode (∅ 49 mm). Two materials tested were the ceramics D (thickness 3 mm) and the coating F (thickness 3 mm) consisting of particle chains of MgO and made by electrostatics coating [8].

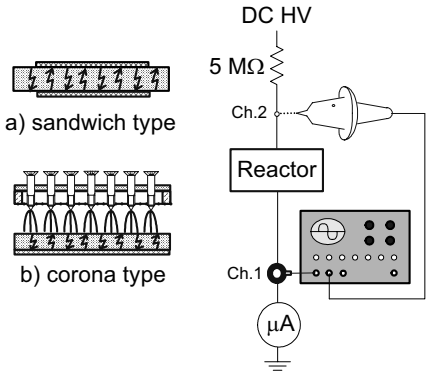

Fig. 1. Experimental apparatus.

Ceramics	Al_2O_3 Contents [%]	Pore Size [μm]	Porosity [%]
A	99	0.8	38
B	92	15	42
C	92	90	37
D	n/a	800	80~90
E	n/a	1250	80~90

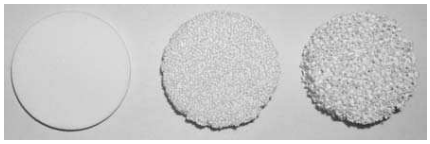

Fig. 2. Properties and shapes of the used dielectric materials (from left to right B, D, E).

DC regulated high voltage power supply (Pulse Electronic Engineering, M502), connected via a 5 MΩ series resistor to limit the total discharge current, was used to drive the

discharge reactor. The discharge of positive polarity was investigated only. The voltage was measured by a high voltage probe (Tektronix, P6015A) and the discharge current and the current pulses were measured using a current probe (Tektronix, P6021) linked to the digitizing oscilloscope (Tektronix, TDS644A). The photographs of discharge were taken by the digital camera (Nikon, E4300) with adjustable iris and exposure time. All experiments were carried out in atmospheric air at 21 °C and 60 % relative humidity.

3 Experimental results

The pore size was found to be the most critical parameter for the microdischarge generation. The Fig. 3 represents the I–V characteristic of the discharge using the ceramics A in the sandwich geometry (full circles). At very low currents (less than 100 μA), the I–V characteristic was relatively stable in time. With further increase of the discharge voltage, the current increased but was not stable and had a tendency to decrease spontaneously in time. As a result, the I–V curve bent. This effect can be most likely assigned to the dielectric layer of high resistivity between the electrodes, as the charge emitted from the active electrode is accumulated on its surface. The accumulated charge increases the potential difference on the dielectric layer and decreases the potential in the gap [9]. The electric field in the gap is thus smaller and the current decreases. Fig. 4 presents the spontaneous decrease of the discharge current and the simultaneous increase of the voltage across the gap in time. During one minute, the discharge current of 1 mA (1.8 kV) spontaneously decreased to only 160 μA (5.3 kV). Empty circles in Fig. 3 represent the I–V characteristic that bears the information about the spontaneous decrease of the current and its saturated values.

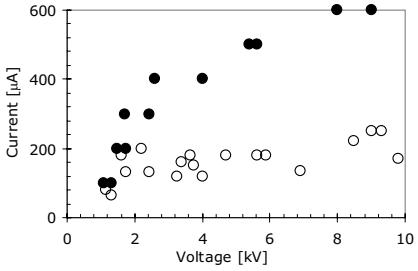

Fig. 3. The I–V characteristic for ceramics A in sandwich geometry.

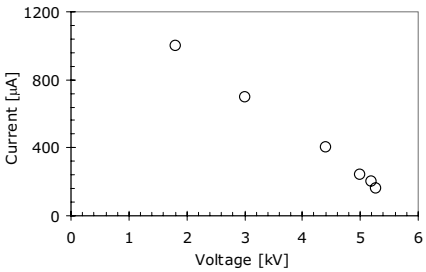

Fig. 4. Spontaneous decrease of current in time for ceramics A in sandwich geometry.

The changes in the electrical characteristic of the ceramics A were accompanied with the changes in the visual discharge character. Fig. 5 shows the photographs of the discharge. The pictures were taken at the balanced current of 200 μA and increasing discharge voltage. The pictures (a–c) were taken with 8 seconds shutter speed. The last two pictures (c–d) represent the identical discharge, taken with 8 and 1 second shutter speed, respectively, to evaluate the effects of shutter speed. The small pores of ceramics A caused the discharge streamers developed and propagated along the surface of the dielectric layer.

The streamers inside the porous dielectric were not observed. Increasing the discharge current/power resulted only in the extension of the area covered by surface streamers.

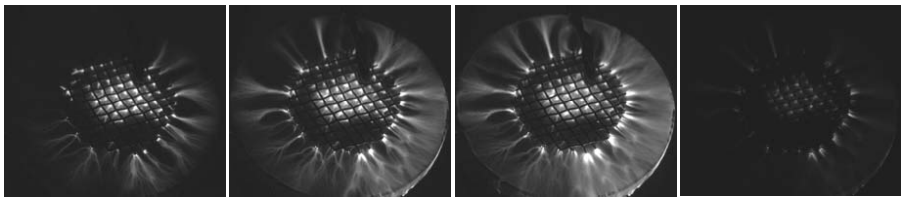

Fig. 5. Visual character of the discharge using ceramics A – current: 200 μA, increasing discharge voltage, shutter speed: 8 s (a–c) and 1 s (d).

For the ceramics B, the discharge character at low discharge currents was similar to ceramics A. The enhanced perforation and bigger pore size of the ceramics B caused, however, that from a certain point the discharge characteristic and its mode changed. In addition to the surface streamers, space streamers inside the porous material developed simultaneously. The blue color changed into intense white light emission, as many randomly distributed microdischarges formed. The series of photographs in Fig. 6 represents the discharge development from surface streamers into microdischarges inside the porous ceramics. The discharge light emission is not homogenous as can be thought looking at Fig. 6c, but the channels migrate and are rather randomly distributed in time and space.

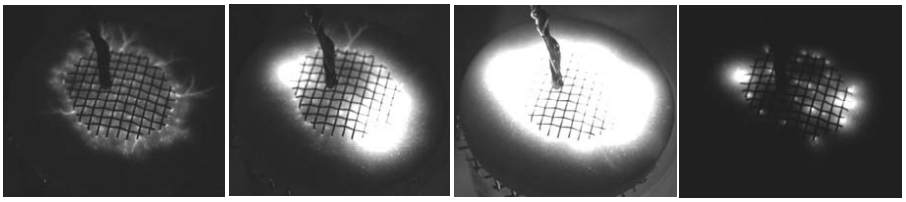

Fig. 6. Visual character of the discharge using ceramics B – current: 200 μA, increasing discharge voltage, shutter speed: 8 s (a–c) and 1 s (d).

Regarding the discharge electrical properties, the onset and working voltages increased compared with the ceramics A. The I–V characteristic was similar to the ceramics A, i.e. relatively stable at low currents, with tendency to bent with increasing discharge voltage (empty circles in Fig. 7). Increasing the applied voltage further, the discharge mode in a certain moment changed as many microdischarges developed inside the porous ceramic (Fig. 6b). The voltage drop during the discharge pulses was significant, some 80÷90 % of the applied voltage. The I–V characteristic became positive and the discharge current stabilized in time (full triangles in Fig. 7).

Figs. 8 and 9 summarize the experimental results obtained using ceramic materials A, B, 2B (B of double thickness), C, 2C and D. Fig. 8 represents the I–V characteristics of the discharges prior to microdischarge formation. The onset and working voltages increased with the pore size and thickness of the ceramics. As mentioned before, no microdischarge generation was observed for ceramics A, due to the very small pores. Us-

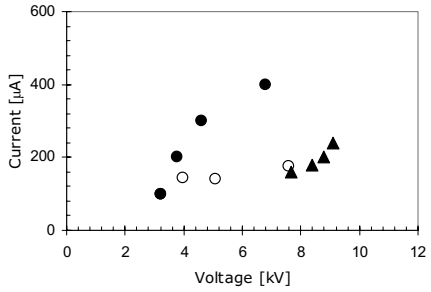

Fig. 7. The I–V characteristic for ceramics B in sandwich geometry.

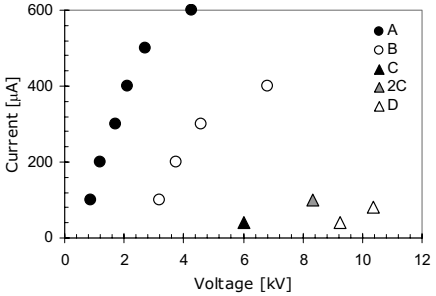

Fig. 8. The I–V characteristics of the discharges other than microdischarge in sandwich geometry.

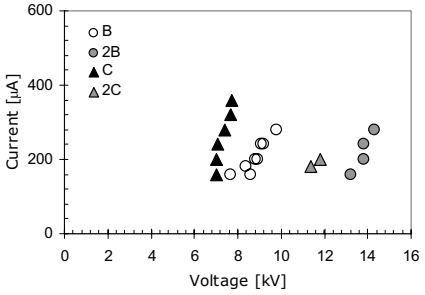

Fig. 9. The I–V characteristics of the microdischarge in sandwich geometry.

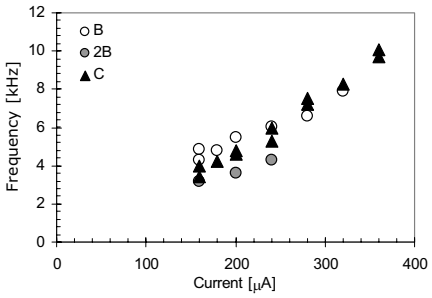

Fig. 10. Frequency of the microdischarge pulses dependent on the discharge current in sandwich geometry.

ing the ceramics D and E, the microdischarges were not formed either. Due to the big pore size their surface could not be effectively charged, and therefore a rapid and almost immediate spark breakdown followed almost right after the discharge onset. It turns out that the microdischarges can be generated only for a certain pore size and above a certain discharge voltage. Fig. 9 summarizes the I–V characteristics of the microdischarges using ceramics B, 2B, C and 2C. The bigger the pores, the lower voltage is needed for microdischarges to be formed. The frequency of the pulses varied between 4÷10 kHz, depending on the discharge current, however appears to be independent on the pore size (Fig. 10).

The obtained results are in a good agreement with the estimates from the Paschen's law, which determines the breakdown voltage of a uniform electric field between planar electrodes as a function of the pressure and the gap length. At atmospheric pressure, the Paschen's minimum is below several micrometers in air, which is about the size of pores of the ceramics where microdischarges generation was confirmed.

The microdischarge generation was also investigated in corona discharge reactor with a grounded electrode covered or coated by a dielectric layer. Three different configurations –

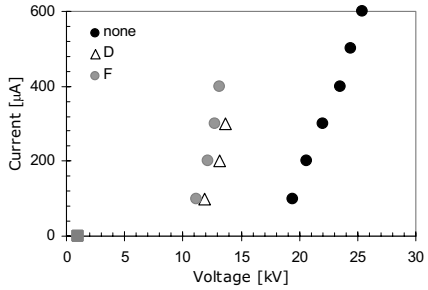

Fig. 11. The I–V characteristic in corona geometry.

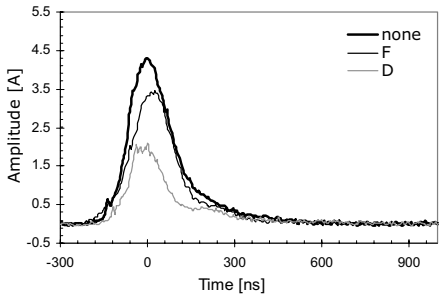

Fig. 12. The current pulse waveforms in corona geometry – current: 400 μA).

no dielectric, ceramics D and coating F – were tested and I–V characteristics, current pulse waveforms and discharge photographs were recorded. Figs. 11 and 12 show I–V characteristics and current pulse characteristics of the discharge, respectively, with and without dielectric layer. With the layer, the onset voltage was lower and the discharge current increased at the given applied voltage. A decrease of the amplitude of the current pulses was observed too. To confirm the active role of either porous ceramics D or coating F, a perforated Teflon sheet with 1 mm thickness was placed on the metal electrode. No change in either I–V characteristic or current pulse characteristic was found in such case. Therefore, we assume the dielectric layers D and F play an active role in the process and the decrease of the working voltage and amplitude of the pulses is a result of the interplay between corona discharge in space and microdischarges inside the pores. During the current pulse, the voltage across the reactor dropped for about 15÷20 % only (at 400 μA). The voltage drops in corona and sandwich geometries cannot be, however, compared since in the corona case, it is the product of two different discharges, i.e. streamer discharge in space and the microdischarges inside the ceramics.

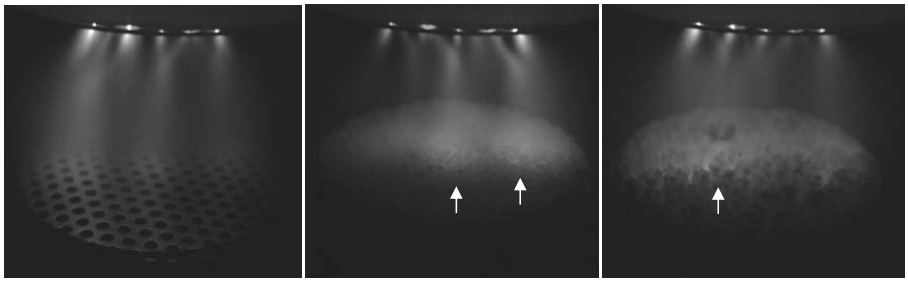

Fig. 13. Visual character of the discharge in corona geometry – materials: a) no dielectric, b) ceramic D, c) coating F, current: 400 μA, shutter speed: 8 s.

The photographs of the discharge are presented in Fig. 13. When no dielectric or Teflon sheet covered the electrode surface the only light emission came out of the space between the electrodes. However, when either ceramics D or coating F layers were present, several

smaller or bigger shining areas (marked by the arrows in the figure) were observed on the surface. We assume that these are probably where many microdischarges are formed.

4 Conlusions

The generation of microdischarges inside the dielectric porous materials by dc power was investigated. It was shown that the pore size is the most critical parameter for the microdischarges to occur. In the sandwich geometry, microdischarges cannot be observed if ceramics pores are smaller than 1 μm or bigger than several hundreds of μm. Stable microdischarges was effectively generated with ceramics of the average pore size of 1÷100 μm (ceramics B and C) and above the certain applied voltage. The spark breakdown is suppressed due to cooling of microdischarge channels by heat-resistive ceramic pores. The frequency of the microdischarges is in the kHz order and is relatively independent on the pore size. In the corona geometry the microdischarges are generated along with the streamer discharge between the electrodes.

We believe the microdischarges generated inside the porous materials can be very effectively used for the gas treatment. In addition to the presented results, we investigated the effect of water vapor on the microdischarge generation and evaluated the efficiency of ozone generation. These results are reported elsewhere [10].

This work was supported in part by the 21st Century COE program "Ecological Engineering for Homeostatic Human Activities" of Ministry of Education, Culture, Sports, Science and Technology, Japan and within the VEGA project 1/0256/03 of Scientific Grant Agency of Ministry of Education, Slovak Republic.

References

[1] H. H. Kim, G. Prieto, K. Takashima, S. Katsura, A. Mizuno: J. Electrostat. **55** (2002) 25.

[2] K. Urashima, J.S . Chang: IEEE T. Dielect. El. In. **7** (2002) 602.

[3] F. Holzer, U. Roland, F. K. Kopinke: Appl. Catal. B **38** (2002) 163.

[4] T. Yamamoto, M. Okubo, T. Nagaoka, K. Hayakawa: IEEE T. Ind. Appl. **38** (2002) 1168.

[5] A. Ohsawa, R. Morrow, A. B. Murphy: J. Phys. D. Appl. Phys. **33** (2000) 1487.

[6] X. Xu: Thin Solid Films **390** (2001) 237.

[7] H. H. Kim: *Application of Non-thermal Plasma in Environmental Protection*, PhD Thesis, Toyohashi University of Technology, Toyohashi, 2000.

[8] G. Li, K. Takashima, S. Katsura, A. Mizuno: J. Inst. Electrostat. Jpn. **28** (2004) 133.

[9] A. Jaworek, A. Krupa, T. Czech: J. Phys. D. Appl. Phys. **29** (1996) 2439.

[10] Y. Matsui, K. Hensel, K. Takashima, S. Katsura, A. Mizuno: in *Proc. of International COE Forum on Plasma Science and Technology* (Edited by N. Sakai), Nagoya University, Nagoya, 2004, 65.